fermentation

Article

Performance and Bacterial Characteristics of Aerobic Granular Sludge in Treatment of Ultra-Hypersaline Mustard Tuber Wastewater

Jingxue Yue [1,2], Xushen Han [1,2,*], Yan Jin [2] and Jianguo Yu [1,2,*]

1 State Environmental Protection Key Laboratory of Environmental Risk Assessment and Control on Chemical Process, East China University of Science and Technology, 130 Meilong Road, Shanghai 200237, China
2 National Engineering Research Center for Integrated Utilization of Salt Lake Resources, East China University of Science and Technology, 130 Meilong Road, Shanghai 200237, China
* Correspondence: xushen.han@ecust.edu.cn (X.H.); jgyu@ecust.edu.cn (J.Y.)

Abstract: Mustard tuber wastewater (MTW) is an ultra-hypersaline high-strength acid organic wastewater. Aerobic granular sludge (AGS) has been demonstrated to have high tolerance to high organic loading rate (OLR), high salinity, and broad pH ranges. However, most studies were conducted under single stress, and the performance of AGS under multiple stresses (high salinity, high OLR, and low pH) was still unclear. Herein, mature AGS was used to try to treat the real MTW at 9% salinity, pH of 4.1–6.7, and OLR of 1.8–7.2 kg COD/m^3·d. The OLR was increased, and the results showed that the upper OLR boundary of AGS was 5.4 kg COD/m^3·d (pH of 4.2) with relatively compact structure and high removal of TOC (~93.1%), NH_4^+-N (~88.2%), and TP (~50.6%). Under 7.2 kg COD/m^3·d (pH of 4.1), most of the AGS was fragmented, primarily due to the multiple stresses. 16S rRNA sequencing indicated that *Halomonas* dominated the reactor during the whole process with the presence of *unclassified-f-Flavobacteriaceae*, *Aequorivita*, *Paracoccus*, *Bradymonas*, and *Cryomorpha*, which played key roles in the removal of TOC, nitrogen, and phosphorus. This study investigated the performance of AGS under multiple stresses, and also brought a new route for highly-efficient simultaneous nitrification–denitrifying phosphorus removal of real MTW.

Keywords: mustard tuber wastewater; MTW; hypersaline wastewater; aerobic granular sludge; AGS; organic loading rate; OLR; simultaneous nitrification–denitrifying phosphorus removal; SNDPR; 16S rRNA sequencing

check for updates

Citation: Yue, J.; Han, X.; Jin, Y.; Yu, J. Performance and Bacterial Characteristics of Aerobic Granular Sludge in Treatment of Ultra-Hypersaline Mustard Tuber Wastewater. *Fermentation* **2023**, *9*, 224. https://doi.org/10.3390/fermentation9030224

Academic Editors: Shamas Tabraiz and Evangelos Petropoulos

Received: 9 February 2023
Revised: 23 February 2023
Accepted: 24 February 2023
Published: 26 February 2023

1. Introduction

Chinese Zhacai (pickled mustard tuber) is one of the three most famous pickles in the world [1]. During the pickled mustard tuber production process, large amounts of mustard tuber wastewater (MTW) were produced in the pickled and pos-process (washing, desalination, dewatering, and sterilization) [2]. MTW has been reported as a typical hypersaline high-strength organic wastewater with 2.5–20% of salinity, 0.3–25 g/L of organic pollutants, 0.5–7 g/L of suspended solid, high concentrations of nitrogen and phosphorus, and low pH (3.7–6.6) [1,3–5].

Although high salinity inhibits microbial metabolism [5–7], biological methods have shown potential in treating MTW [1,5]. Due to the high salinity, the conventional activated sludge method was easy to collapse and the biofilm method became the mainstream process, in which sequencing batch biofilm reactor (SBBR) and biofilm-membrane bioreactor (BMBR) were frequently used. Chen et al. [8,9], Liu et al. [6], and Wang et al. [5] used SBBR to treat 7% salinity MTW, and high chemical oxygen demand (COD) removal efficiency was reached under high organic loading rate (OLR) (0.5, 3.0, and 0.9 kg COD/m^3·d). In parallel, 7% and 10% salinity MTW were treated by BMBR, and 72.1% and 85.6% of COD removal efficiency were achieved under 3.0 and 3.3 kg COD/m^3·d, respectively [4,7]. However, the addition of fillers in SBBR and BMBR increased costs and brought in sludge disposal and environmental pollution problems. Moreover, the more serious membrane fouling problems under high salinity hindered the application of BMBR [4,7,10].

Aerobic granular sludge (AGS) is a type of granular sludge formed by self-immobilization of microorganisms, and has many advantages, such as excellent settling velocity, high OLR tolerance, good shock resistance, small area, and low cost [11,12]. To date, few studies were found to use AGS technology for the treatment of real MTW, primarily due to its extremely high salinity and low pH. However, it has been demonstrated that AGS technology had better simultaneous nitrogen and carbon removal efficiency in hypersaline high-strength organic wastewater treatment [13]. For instance, Moussavi et al. [14] and Ibrahim et al. [15] reported a high COD removal efficiency (99% and 90%) of AGS in hypersaline wastewater (8% and 8.5%) treatment under 1.7 and 2.7 kg COD/m^3·d, respectively. In addition, high total organic carbon (TOC), total nitrogen (TN), and total phosphorus (TP) removal efficiency (93%, 98%, and 97%) were reached under 12% salinity using AGS [16]. Meanwhile, Corsino et al. [17] used AGS to reach high TOC and TN removal (90% and 40%) in 7.5% salinity fish canning wastewater under 4 kg COD/m^3·d.

Our previous study has demonstrated AGS could maintain high TOC removal under 3% salinity and influent pH of 5.0 [13]. Additionally, we directly cultivated salt-tolerant aerobic granular sludge (SAGS) under 9% salinity and had perfect organic removal efficiency under 9.9 kg COD/m^3·d. Based on these results, we found AGS possessed the potential of high tolerance to high OLR, high salinity, and low pH. Accordingly, herein, MTW was treated by using AGS technology, to show its potential in real hypersaline high-strength acid organic wastewater treatment with multiple stresses.

In this study, salt-tolerant aerobic granular sludge (SAGS) was used to treat hypersaline (9% salinity) MTW, and the OLR was increased in a stepwise manner (1.8 – 7.2 kg COD/m^3·d) with decreased pH (4.1–6.7) during the treatment process. SAGS characteristics and organic pollutants (C, N, and P) removal performance were investigated, and high-throughput sequencing was applied to explore the microbial community affected by real MTW under high OLR. This study aimed to investigate: 1) the potential of SAGS to treat real MTW; and 2) the performance of SAGS in hypersaline MTW under high OLR and low influent pH. This study explored the performance of AGS under multiple stresses in real MTW.

2. Materials and Methods

2.1. Inoculum and Wastewater Characteristics

The mature SAGS was collected from another sequencing batch reactor (SBR) that ran under 9% salinity for 135 days, and it was inoculated to the new SBR with initial mixed liquid volatile suspended solids (MLVSS) of 3.0 g/L. Real wastewater was taken from Jixiangju Food Co., Ltd. (Meishan, Sichuan, China). The characteristics of wastewater, and the kinds and concentrations of organic acids are shown in Table 1 and Table S1. The wastewater was diluted with fresh water and the salinity was adjusted to 9% by adding NaCl to be used as influent. The influent pH was not adjusted to maintain an acidic environment.

2.2. Reactor Set-Up and Operation

A SBR was used for the experiment with a working volume of 4.0 L (inner diameter of 8 cm) and operated for 20 days. The cycle time was 8 h, including feeding time (0.083 h), settling time (0.05 h), aeration time (7.78 h), and discharging time (0.083 h). A volume exchange ratio (VER) of 60% was fixed, and OLR was improved by decreasing the dilution rate. The air velocity was adjusted when OLR changed (Table 2). More details about the reactor could be found in Tang et al. [18]. The operational temperature was maintained at 23 ± 2 °C while the pH was not adjusted and controlled.

Table 1. Characteristics of mustard tuber wastewater.

Parameter	Value
TOC (mg/L)	9600
COD (mg/L)	33,275
TN (mg/L)	1328
NH_4^+-N (mg/L)	794
NO_3^--N (mg/L)	90
NO_2^--N (mg/L)	2
Organic nitrogen (mg/L)	442
TP (mg/L)	378
pH	3.78
Conductivity (ms/cm)	152
Cl^- (mg/L)	68,600
Salinity (mg NaCl/L)	113,000

Table 2. Composition of influent wastewater and operation conditions.

Period	Operational Day (d)	Influent COD (mg/L)	Dilution	OLR (kg COD/m^3·d)	Air Velocity (cm/s)
I	1–5	1000	3:100	1.8	1.2
II	6–10	2000	6:100	3.6	1.8
III	11–15	3000	9:100	5.4	2.4
IV	16–20	4000	12:100	7.2	3.0

2.3. Analytical Methods

The morphology and microstructure of sludge were observed by the camera, stereoscopic microscope (SteREO Discovery.V20, ZEISS, Germany), and scanning electron microscopy (SEM) (Quanta FEG 650, ThermoFisher, USA), respectively [18]. Energy dispersive spectroscopy (EDS) (Quantax XFlash 6-30, Bruker, Germany) was used to analyze the elements inside SAGS. The particle size of SAGS was recorded by image software (ImageJ.JS, v0.5.5). Dissolved oxygen (DO) concentration and pH were detected by a portable water quality analyzer (HQ40d, Hach, USA). The concentration of TOC was analyzed by a TOC analyzer (Sievers InnovOx Laboratory, SUEZ, USA) in case of the large deviation of COD detection under high salinity conditions [18]. Mixed liquid suspended solids (MLSS), MLVSS, sludge volume index (SVI_5 and SVI_{30}), NH_4^+-N, NO_3^--N, NO_2^--N, TN, and TP were analyzed based on the standard methods [19].

The organic acids in the MTW were detected by the high performance ion chromatography (HPIC) (ICS-6000, ThermoFisher, USA) equipped with Dionex IonPac^{TM} AS11-HC (9 µm, 4 × 250 mm) and a conductivity detector. The mobile phase was KOH solution, and gradient elution was performed at a flow rate of 1.0 mL/min.

2.4. High-Throughput Sequencing (16S rRNA) Analysis

Sludge samples were collected and stored at −80 °C, and DNA was extracted from these samples using FastDNA®Spin Kit for Soil (MP Biomedicals, USA). Then, the extracted DNA was checked for concentration and quality using NanoDrop 2000 UV-vis spectrophotometer (Thermo Scientific, Wilmington, USA) and 1% agarose gel.

The primer pairs 338F/806R were used to amplify the V3–V4 regions of the bacterial 16S rRNA gene. After purification and quantification, the PCR amplicons were used to build Miseq library. Then, sequencing was conducted by an Illumina MiSeq PE300 platform (Illumina, San Diego, USA) by Majorbio Bio-Pharm Technology Co., Ltd. (Shanghai, China). The raw data was uploaded to the NCBI SRA database (Accession Number: PRJNA918964). Operational taxonomic units (OTUs) with 97% similarity cutoff were obtained using UPARSE, and chimeric sequences were removed.

3. Results and Discussions

3.1. The Organic Removal Performance of SAGS

To explore the pollutants removal performance of SAGS for real MTW, the mature SAGS was inoculated in the SBR with real MTW (9% salinity, pH 4.1–6.7) as influent. The treatment process was divided into four periods according to different OLRs.

The removal performance of AGS in the MTW was first evaluated (Figure 1). In Period I (1.8 kg COD/m^3·d), TOC removal efficiency increased gradually from 86.1% to 91.2% (Figure 1A), indicating the SAGS was adapted to the MTW gradually. Furthermore, the organic acids (lactic acid, acetic acid, propionic acid, succinic acid, citric acid, and oxalic acid) in the wastewater were easily degradable, resulting in high TOC removal efficiency. While the NH_4^+-N removal efficiency was decreased from 95.9% to 65.2% (Figure 1B), which might be because the low influent pH affected the N removal efficiency of SAGS [13]. At the same time, low concentrations of NO_2^--N (0–0.4 mg/L) and NO_3^--N (0–1.1 mg/L) were detected in the effluent (Figure 1C), indicating that the simultaneous nitrification and denitrification process occurred. The TP removal efficiency was increased first and then decreased (Figure 1D). The average TP removal efficiency was 30.3%.

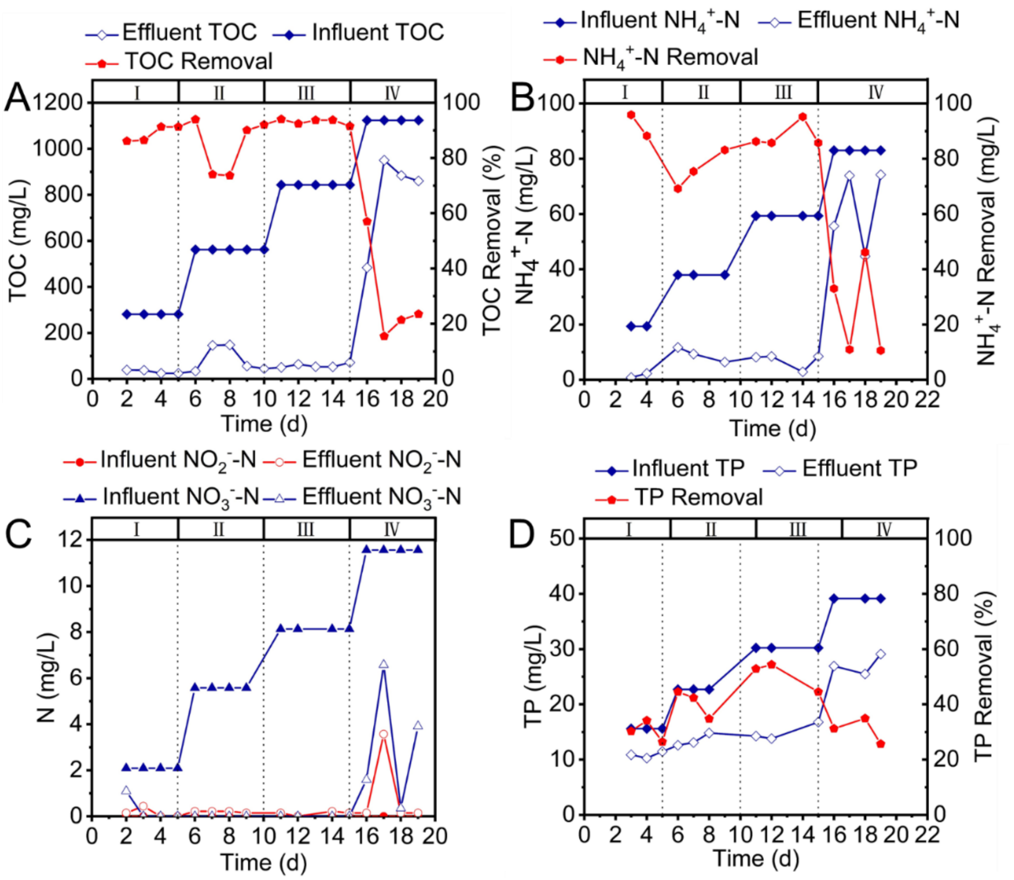

Figure 1. The pollutants removal performance of mustard tuber wastewater: (**A**) TOC; (**B**) NH_4^+-N; (**C**) NO_2^--N and NO_3^--N; (**D**) TP. Period I: 1.8 kg COD/m^3·d; Period II: 3.6 kg COD/m^3·d; Period III: 5.4 kg COD/m^3·d; Period IV: 7.2 kg COD/m^3·d.

In the subsequent Period II (3.6 kg COD/m^3·d), the TOC removal efficiency had a sharp decline of 74% on Day 7 and Day 8 and then recovered to 90.0% on Day 9 (Figure 1A). The NH_4^+-N removal efficiency began to rise from 69.2% to 83.1% (Figure 1B), and the concentrations of NO_2^--N (0.1–0.2 mg/L) and NO_3^--N (0 mg/L) in the effluent maintained a low level (Figure 1C), indicating the microorganisms related to nitrogen removal were adapted to the wastewater and N removal performance improved gradually. The average TP removal efficiency was further increased to 40.5% (Figure 1D).

In the following Period III (5.4 kg COD/m^3·d), the TOC removal efficiency maintained stable at a high level (Figure 1A). The NH_4^+-N removal efficiency continued to grow up to 95.2% (Figure 1B), and almost no NO_2^--N (0.1–0.2 mg/L) and NO_3^--N (0 mg/L) were present in the effluent (Figure 1C). The TP removal efficiency continued to increase to 50.6% (Figure 1D), indicating the SAGS had good P removal ability.

In the final Period IV (7.2 kg COD/m^3·d), the TOC removal efficiency sharply declined to 15.5%, and then had a limited increase (Figure 1A). Furthermore, the NH_4^+-N removal efficiency had a sudden decrease and fluctuation (Figure 1B). The concentrations of effluent NO_2^--N (0.1–3.6 mg/L) and NO_3^--N (0.3–6.6 mg/L) were increased and unstable (Figure 1C). At the same time, the concentrations of effluent TP increased and the TP removal efficiency decreased from 31.2% to 25.6% (Figure 1D). All the indexes indicated that the organic removal performance became poor and the SAGS system collapsed (Figures 1–3).

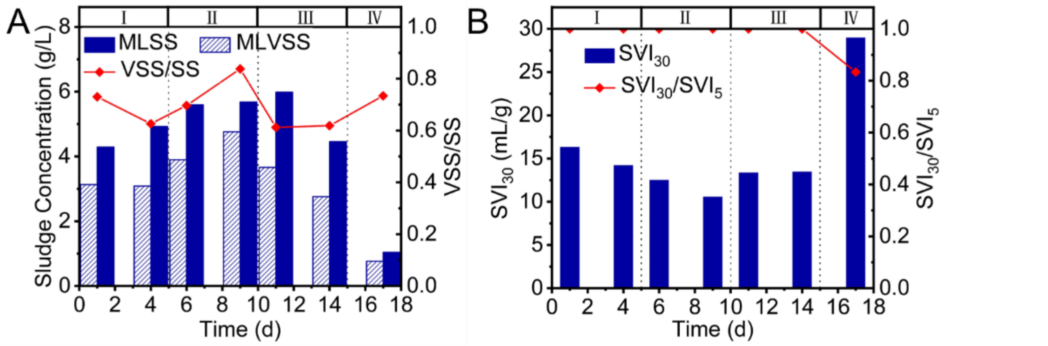

Figure 2. Sludge characteristics of SAGS: (**A**) MLSS, MLVSS, and VSS/TSS; (**B**) SVI_{30} and SVI_5/SVI_{30}. Period I: 1.8 kg COD/m^3·d; Period II: 3.6 kg COD/m^3·d; Period III: 5.4 kg COD/m^3·d; Period IV: 7.2 kg COD/m^3·d.

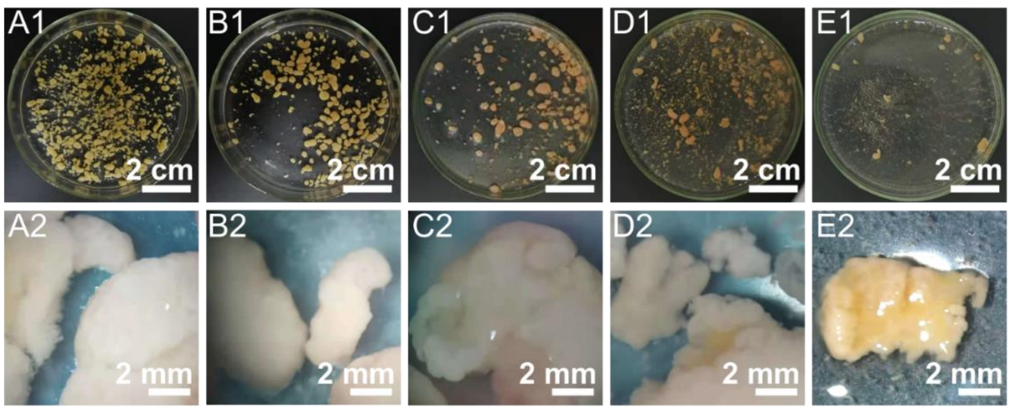

Figure 3. SAGS morphology under different OLR: (**A**) Initial; (**B**) Period I (1.8 kg COD/m^3·d); (**C**) Period II (3.6 kg COD/m^3·d); (**D**) Period III (5.4 kg COD/m^3·d); (**E**) Period IV (7.2 kg COD/m^3·d). (**A1**–**E1**) were taken by a camera, and (**A2**–**E2**) were taken by stereoscopic microscope.

In conclusion, the SAGS had good organic removal performance in real hypersaline MTW with low pH (4.2–6.7) under 1.8–5.4 kg COD/m^3·d. The TOC and NH_4^+-N removal performance could maintain ~88.9% (73.7–94.0%) and ~85.0% (69.2–95.9%), respectively. The concentrations of effluent NO_2^--N (0.1–0.4 mg/L) and NO_3^--N (0 mg/L) were always low, indicating good TN removal performance. The average TP removal performance was about 40.5% (26.4–54.4%) and the maximum could reach 54.4% under 55.2 g P/m^3·d without sludge discharge. The P might be removed by phosphorus-accumulating organisms (PAOs), microbial assimilation, the accumulation in the extracellular polymeric substances (EPS), or the formation of phosphate precipitation [20,21]. When the OLR increased to

7.2 kg COD/m^3·d, the system collapsed, indicating the upper OLR boundary was 5.4 kg COD/m^3·d for MTW treatment without adjustment of influent pH (~4.2).

Over the past years, biofilm technologies, such as SBBR and BMBR, were used as the main biological methods for treatment of MTW [4–8], while AGS was rarely used. Therefore, the comparison of these biological treatment technologies in the hypersaline (≥7%) MTW treatment was shown in Table 3. The range of OLR that SBBR had high removal efficiency was 0.5–3.0 kg COD/m^3·d under 7% salinity [5,6,8], and BMBR technology had high removal efficiency under higher OLR of 3.0–3.3 kg COD/m^3·d and 7–10% salinity [4,7]. It is worth noting that AGS technology could operate with excellent removal performance under higher OLR of 5.4 kg COD/m^3·d and 9% salinity. These results indicated that AGS was more suitable for the treatment of ultra-hypersaline high-strength acid organic wastewater.

Table 3. The OLR and removal performance of different biological treatment technologies in the treatment of ultra-hypersaline (≥7%) MTW.

Technology	Salinity (%)	OLR (kg COD/m^3·d)	Removal Performance	Reference
SBBR	7	0.5	90.2–91.9% of COD removal; 65.5% of phosphate removal	[8]
SBBR	7	3.0	87.9% of COD removal	[6]
SBBR	7	0.9	85.2% of COD removal; 98.6% of TN removal	[5]
BMBR	10	3.3	85.6% of COD removal; 60.4% of TN removal	[7]
BMBR	7	3.0	72.1% of COD removal; 74.0% of NH_4^+-N removal; 20% of SP removal	[4]
AGS	9	5.4	93.1% of TOC removal; 88.2% of NH_4^+-N removal; 50.6% of TP removal	This study

Previous studies found that the upper OLR boundary that AGS could maintain high organic pollutants removal efficiency was 27.0, 14.4, and 8.1 kg COD/m^3·d, respectively under the salt-free, 3% salinity, and 9% salinity conditions [13,22]. Therefore, it could be deduced that the upper OLR boundary of AGS was related to salinity with a negative correlation, which might be because the salinity inhibited the metabolic rates of microorganisms [5–7]. Since the acid environment could inhibit the organic pollutants removal efficiency [13], the upper OLR boundary was further reduced to 5.4 kg COD/m^3·d in the mustard tuber wastewater with 9% salinity in this study.

3.2. The Sludge Characteristics of SAGS

3.2.1. The Sludge Properties of SAGS

The sludge characteristics of SAGS were also shown in Figure 2. During Period I and Period II (OLR = 1.8–3.6 kg COD/m^3·d), the MLVSS increased from 3.1 to 4.8 g/L and MLSS increased from 7.4 to 10.4 g/L gradually (Figure 2A). VSS/SS showed the biomass percentage in the sludge and reflected the sludge bioactivity [23,24]. It had a little decrease from 0.73 to 0.63 and then increased to 0.84 (Figure 2A), indicating the sludge bioactivity was increased with the increased OLR after adaptation. At the same time, the SVI_{30} kept decreasing from 16.3 to 10.6 mL/g, and SVI_{30}/SVI_5 = 1 (Figure 2B), indicating a denser granular structure with a certain high OLR, which was also observed in other studies [25,26].

In Period III (5.4 kg COD/m^3·d), the MLVSS and MLSS had a drop to 2.8 and 7.2 g/L, respectively. VSS/SS was also decreased from 0.84 to 0.61 (Figure 2A), indicating sludge bioactivity was declined. The SVI_{30} had a little increase but was still lower than the initial value (Figure 2B) and SVI_{30}/SVI_5 was still 1 (Figure 2B). All the indexes reflected the SAGS became unstable, although the air velocity was enough (Table 1).

In Period IV (7.2 kg COD/m^3·d), the MLVSS and MLSS continued to decrease to 0.8 and 1.0 g/L, but VSS/SS increased (Figure 2A), which might be because the inorganic substances were discharged with effluent after fragmentation (Figure 3E). SVI_{30} was increased from 13.5 to 29.0 mL/g, and SVI_{30}/SVI_5 was decreased from 1 to 0.83 (Figure 2B), indicating that the structure of SAGS became loose.

Overall, the SAGS could maintain high sludge concentration, high sludge bioactivity, and dense and intact structure under 1.8–5.4 kg COD/m^3·d in real MTW. However, fragmentation occurred when OLR was 5.4 kg COD/m^3·d, and then the SAGS system collapsed under 7.2 kg COD/m^3·d.

3.2.2. The Sludge Morphology of SAGS

The sludge morphology was also recorded at the end of each period (Figure 3). During Period I and Period II, the SAGS could maintain intact structure (Figure 3(A1–C1)) with an increased particle size (from 2195 to 2830 μm), but many small protrusions emerged on the surface of SAGS (Figure 3(C2)) from Period II, which might be because small granules formed by using inorganic precipitation as core [27]. In Period III, some fragments appeared (Figure 3(D1)), and the small protrusions still existed (Figure 3(D2)). Finally, in Period IV, the SAGS was totally crushed into flocs (Figure 3E). A large amount of sludge was discharged with effluent, and the system collapsed, which were observations consistent with Figures 1 and 2.

The SEM images could further reveal the microscopic changes of microbial communities (Figure 4). Some small protrusions were observed clearly through SEM (Figure 4(A1–D1)), which was similar to Wang et al. [28]. The SAGS was mainly composed of a few fungal hyphae and large amounts of bacteria. A large number of filamentary EPS matrix among microorganisms was observed, which provided a high self-immobilization property for SAGS [29]. In addition, some phosphorus might exist in the EPS, contributing to the high phosphorus removal [20] (Figure 4(A3,B3,C3,D3)). On the surface of the initial SAGS, some gully was observed (Figure 4(A1)), in which some hyphae were not filled with bacteria (Figure 4(A2)). In the subsequent Period I and Period II, the surface structure of SAGS became denser and denser, and some small protrusions appeared (Figure 4B,C), indicating much better sludge properties of SAGS were obtained under certain high OLR, which was consistent with the phenomenon shown in previous studies [25,26]. However, in Period III, a lot of hyphae appeared on the surface of SAGS, and little bacteria was observed on the hyphae (Figure 4D). This indicated that acid environment might inhibit most of the bacteria including AOB, NOB, and PAOs [30–32], and thus it was unbeneficial to the stability of SAGS.

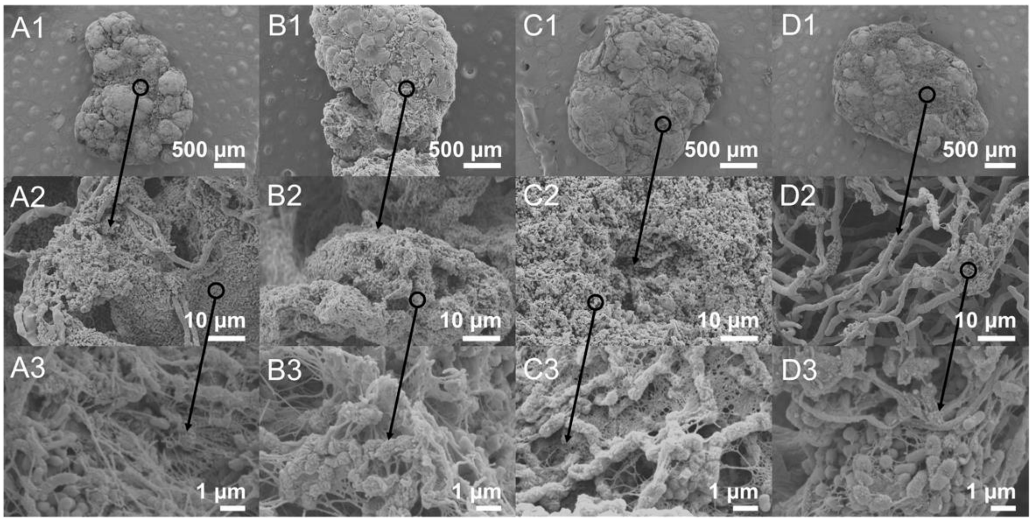

Figure 4. The SEM images of SAGS under different OLR: (**A**) Initial; (**B**) Period I (1.8 kg COD/m^3·d); (**C**) Period II (3.6 kg COD/m^3·d); (**D**) Period III (5.4 kg COD/m^3·d).

Overall, the structure of SAGS was intact and compact under the OLR of 1.8–3.6 kg COD/m^3·d. When OLR increased to 5.4 kg COD/m^3·d, some SAGS fragmented and the proportion of bacteria was decreased due to the acid environment, leading to the final collapse under the OLR of 7.2 kg COD/m^3·d.

3.2.3. The Accumulation of Phosphorus in SAGS

Since a large amount of phosphorus was removed and no sludge was discharged (Figure 1), some phosphorus might have accumulated in SAGS, which increased the inorganic components of SAGS and decreased the bioactivity accordingly (Figure 2) [24]. To further study if the phosphorus accumulated in the SAGS, SEM-EDS was used to analyze the cross section of SAGS (Figure 5).

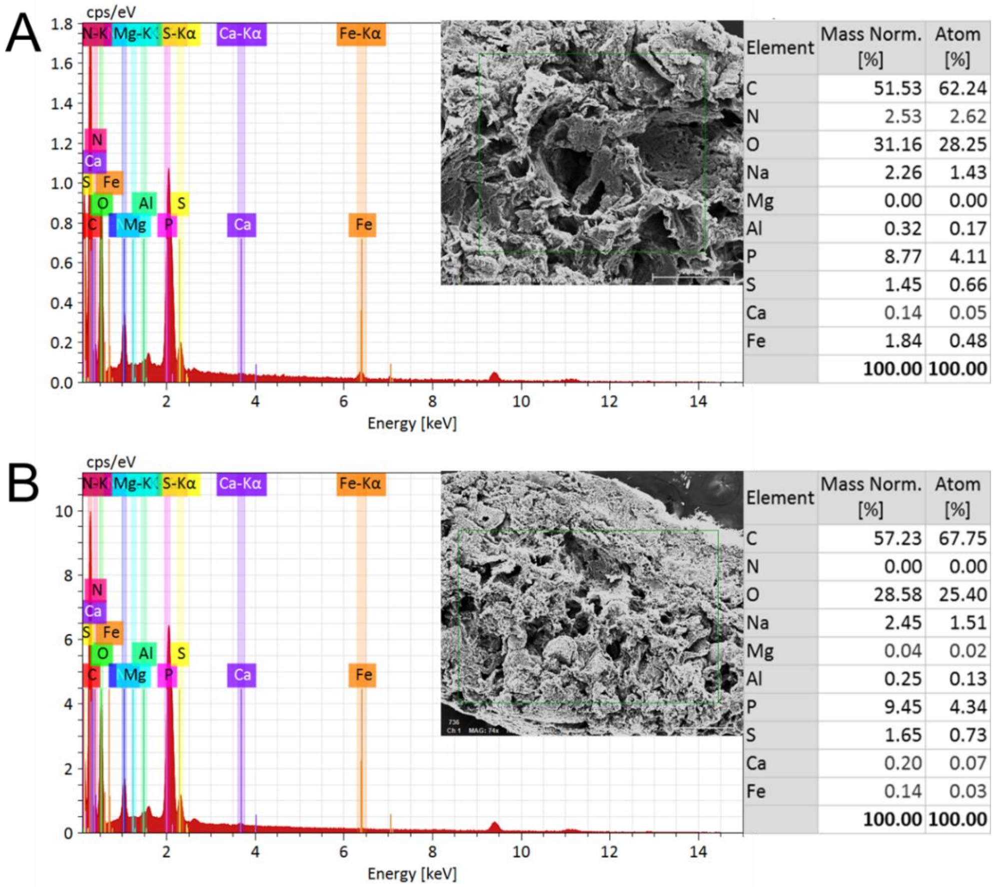

Figure 5. SEM-EDS analysis of the cross section of SAGS (**A**) Initial; (**B**) Period III (5.4 kg COD/m^3·d).

The mass percentage of phosphorus was increased from 8.77% (initial SAGS) to 9.45% (SAGS in Period III), and the mass percentage of Ca was also increased from 0.14% to 0.20%. So, it could be deduced that the phosphorus did accumulate in the granular sludge, and it might exist in the microorganisms, EPS, and inorganic phosphorus precipitation [20,21]. The increase of phosphorus decreased the bioactivity of SAGS (Figure 2) [24], which might lead to the collapse of the SAGS system.

3.3. The Microbial Community of SAGS under Different OLR

The changes in the microbial community were investigated (Table 4 and Figure 6). The alpha diversity analysis was shown in Table 4. ACE and Chao indexes both peaked at 55.94 and 60.00 on Day 5, respectively, which might be because the more complex substrates in the real MTW increased the richness of the microbial community. Then, they decreased to 55.46 and 52.88 with increased OLR, which was also observed in other studies [18,33]. The Shannon and Simpson indexes peaked/bottomed at 1.45/0.42 on Day 10, showing that the diversity of microbial community was increased with the OLR from 1.8 to 3.6 kg COD/m^3·d. Then, they were decreased when OLR was over 3.6 kg COD/m^3·d, indicating a certain high OLR and complex components of wastewater were beneficial to the community diversity, while too high OLR was harmful to the community diversity [18,33].

Table 4. Alpha diversity index of samples on different OLR.

Sample	Sequences	OTUs	ACE [a]	Chao [a]	Shannon [b]	Simpson [c]	Coverage [d]
Day 0	29738	46	49.87	49.50	1.09	0.57	0.9999
Day 5	29738	48	55.94	60.00	1.16	0.53	0.9997
Day 10	29738	51	55.74	55.20	1.45	0.42	0.9999
Day 15	29738	53	55.46	52.88	1.18	0.52	0.9998

[a] Community richness: A higher number represented more richness. [b] Community diversity: A higher number represented more diversity. [c] Community diversity: A lower number represented more diversity. [d] Sampling depth.

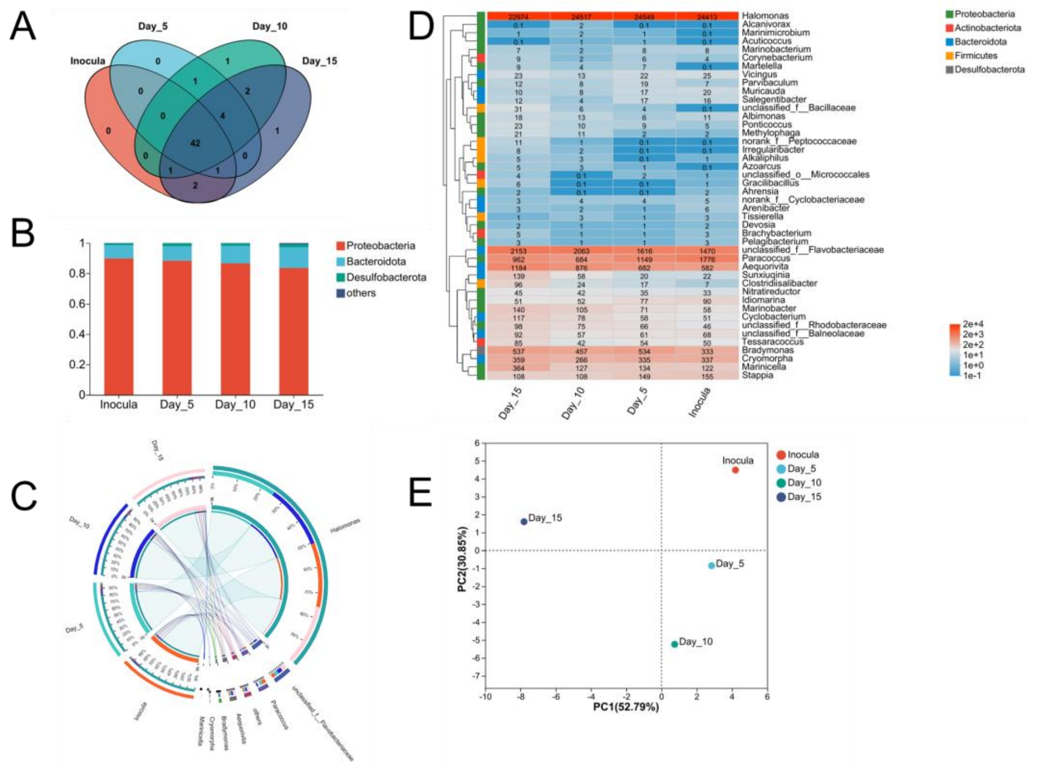

Figure 6. Microbial community structure of SAGS under different OLR. (**A**) Venn diagram on OTU level; (**B**) Barplot analysis on phylum level; (**C**) Circos diagram on genus level; (**D**) Heatmap analysis on genus level; (**E**) PCA on OTU level.

The microbial community difference of SAGS under different OLR was further analyzed (Figure 6A). The number of shared OTU among Inocula, Day 5, Day 10, and Day 15 was 42, which occupied 91.3%, 87.5%, 82.4%, and 80.8% of the total OTU in Inocula, Day 5, Day 10, and Day 15, respectively, indicating the change of influent brought difference for the microbial community, and the increased OLR changed the community to a certain extent.

The community species composition on phylum level was shown in Figure 6B. The microbial community mainly consisted of *Proteobacteria*, *Bacteroidota*, and *Desulfobacterota*, which were found in other salt environments [18,34,35]. *Proteobacteria* dominated the reactor with a decreased proportion of 89.9%, 88.4%, 86.7%, and 83.5%. It was found that *Proteobacteria* could secrete EPS to make SAGS more compact and degrade the organic pollutants [36,37], and its decrease might lead to the instability of the SAGS. *Bacteroidota* accounted for an increasing proportion from 8.7% to 13.8% with the increased OLR. It seemed that *Bacteroidota* was suitable for the environment with high organic acids and also it was reported to be the dominant phylum in pickled vegetables [38]. According to other studies, *Bacteroidota* was related to EPS secretion, and nitrogen and phosphorus removal [39], contributing to the high NH_4^+-N and TP removal efficiency (Figure 1). *Desulfobacterota* accounted for a little proportion (1.1–1.8%), and contributed to desulphurization [40].

The microbial community on genus level was also analyzed (Figure 6C). *Halomonas*, *unclassified-f-Flavobacteriaceae*, *Paracoccus*, *Aequorivita*, *Bradymonas*, *Cryomorpha*, and *Marinicella* were the main genera which were reported in the hypersaline environment [15,41–43]. At the same time, it also reflected that these bacteria could adapt to the severe environment (extremely high salinity and low pH). *Halomonas* was the dominant genus with significantly high relative abundance, which was stable at 82% from Day 0 to Day 10, and was decreased to 77.3% on Day 15. Therefore, it was thought to have the ability to remove organic pollutants [44,45]. The relative abundance of *unclassified-f-Flavobacteriaceae* (4.9–7.2%) and *Aequorivita* (2.0–4.0%) was increased with the increased OLR and belonged to *Bacteroidota* (Figure 6D), indicating *unclassified-f-Flavobacteriaceae* and *Aequorivita* favored the high concentration of organic acids. *Unclassified_f__Flavobacteriaceae* and *Aequorivita* were found to be denitrifying bacteria (DNB) [41,46], whose increase was beneficial for the stability of SAGS and denitrogenation. The proportion of *Paracoccus* was decreased from 6.0% to 3.2%, and *Paracoccus* was found in other biotreatment systems of MTW [47], reflecting that *Paracoccus* was not suitable for high OLR. The relative abundance of *Bradymonas* was increased from 1.1% to 1.8% generally and belonged to *Desulfobacterota* (Figure 6D), indicating it could settle at high OLR and low pH. *Bradymonas* was reported to be able to reduce nitrate to nitrite [42], which helped remove nitrogen. *Cryomorpha* occupied a stable proportion (1.1–1.2%), except for a little drop to 0.9% on Day 10, which was an aerobic chemoheterotroph and could degrade complex organic substances [48]. The relative abundance of *Marinicella* was stable at 0.4% under OLR of 1.8–3.6 kg COD/m^3·d and increased to 1.2% under 5.4 kg COD/m^3·d, indicating it might be a typical bacteria related to the instability of SAGS, although *Marinicella* could utilize sulfide compounds to realize the denitrification function [49]. Furthermore, the relative abundance of *Marinobacter*, *Cyclobacterium*, *unclassified-f-Rhodobacteraceae*, *unclassified-f-Balneolaceae*, *Sunxiuqinia*, *Tessaracoccus*, *Clostridiisalibacter*, and *Nitratireductor* was increased with increased OLR, indicating they favored the high concentration of organic acids and high OLR. While *Stappia* and *Idiomarina* decreased from Day 0 to Day 15, indicating they were not suitable for this environment (Figure 6D).

The response of microbial community structure to different OLR was also analyzed (Figure 6E). The PCA results showed that the microbial community structure of four sludge samples was obviously different, as reflected by the separated points in the figure. Furthermore, the community structure on Day 15 was far different from others, indicating a significant change in the microbial community on Day 15, which was because of the collapse of SAGS. In conclusion, the microbial community changed when OLR increased, especially when OLR was 5.4 kg COD/m^3·d.

Overall, *Halomonas* dominated the reactor during the whole process. Many bacteria had denitrification functions (*unclassified-f-Flavobacteriaceae*, *Aequorivita*, *Paracoccus*, *Marinicella*) and dephosphorization (*unclassified-f-Flavobacteriaceae* and *Aequorivita*), leading to high nitrogen and phosphorus removal. *Unclassified-f-Flavobacteriaceae*, *Aequorivita*, *Bradymonas*, and *Marinicella* favored the environment with the high concentrations of organic acids and high OLR while *Paracoccus* settled at low OLR. Furthermore, the microbial community changed when OLR increased, especially when OLR was 5.4 kg COD/m^3·d.

4. Conclusion

This study investigated the performance of AGS under multiple stresses in real MTW at 9% salinity, pH of 4.1–6.7, and OLR of 1.8–7.2 kg COD/m^3·d using the mature SAGS. The results showed that SAGS could tolerate multiple stresses and treat MTW effectively. The SAGS could withstand a high OLR of 5.4 kg COD/m^3·d after 10 days under low pH (4.2) with relatively compact structure, and the TOC, NH_4^+-N, and TP removal could reach ~93.1%, ~88.2%, and ~50.6%, respectively. Under 7.2 kg COD/m^3·d (pH of 4.1), most of the AGS was fragmented, primarily due to the multiple stresses. The SEM analysis found that acid environment might inhibit most of the bacteria, and thus it was unbeneficial to the stability of SAGS. *Halomonas* dominated the reactor during the whole process with the presence of *unclassified-f-Flavobacteriaceae*, *Aequorivita*, *Paracoccus*, *Bradymonas*, and *Cryomorpha*, which played key roles in the removal of TOC, nitrogen, and phosphorus. This study investigated the performance and bacterial community of AGS under multiple stresses (high salinity, low pH, and high OLR), and also brought a new route for highly-efficient simultaneous nitrification–denitrifying phosphorus removal of real MTW.

Supplementary Materials: The following supporting information can be downloaded at: https://www.mdpi.com/article/10.3390/fermentation9030224/s1, Table S1: The organic acid concentrations of mustard tuber wastewater.

Author Contributions: Conceptualization, J.Y. (Jingxue Yue) and X.H.; data curation, J.Y. (Jingxue Yue); formal analysis, J.Y. (Jingxue Yue) and X.H.; funding acquisition, X.H. and J.Y. (Jianguo Yu); investigation, X.H. and Y.J.; methodology, J.Y. (Jingxue Yue), X.H., and Y.J.; project administration, X.H., Y.J. and J.Y. (Jianguo Yu); resources, X.H., Y.J. and J.Y. (Jianguo Yu); software, J.Y. (Jingxue Yue); supervision, X.H. and J.Y. (Jianguo Yu); validation, X.H. and J.Y. (Jianguo Yu); visualization, J.Y. (Jingxue Yue); writing—original draft, J.Y. (Jingxue Yue); writing—review and editing, X.H. and J.Y. (Jianguo Yu). All authors have read and agreed to the published version of the manuscript.

Funding: This work was sponsored by Shanghai Sailing Program (20YF1409500) and China Postdoctoral Science Foundation (2021T140206, 2021M691010).

Data Availability Statement: Not applicable.

Conflicts of Interest: The authors declare no conflict of interest.

References

1. Xu, L.; Pang, Y.; Liu, W.; Chen, H.; Huang, S.; Zhu, L. Hypersaline Wastewater Produced from Pickled Mustard Tuber (Chinese Zhacai): Current Treatment Status and Prospects. *Water (Switzerland)* **2022**, *14*, 1508. [CrossRef]
2. Xu, L.; Dong, F.; Yang, J.; Liu, W.; Zhu, L.; He, Q.; Wang, X.; Li, H.; Wang, X. Electricity Generation and Acid and Alkaline Recovery from Pickled Waters/Wastewaters through Anaerobic Digestion, Bipolar Membrane Electrodialysis and Solid Oxide Fuel Cell Hybrid System. *Energy Convers. Manag.* **2022**, *251*, 114973. [CrossRef]
3. Chai, H.; Li, S. Investigation of the Removal Efficiency of Foulants by Anoxic/Aerobic Membrane Bioreactor Treating Pickle Wastewater. *Nat. Environ. Pollut. Technol.* **2013**, *12*, 391–396.
4. Kang, W.; Cui, X.; Cui, Y.; Bao, L.; Ma, K. Assessment of High Salinity Wastewater Treatment with Dewatered Alum Sludge-Aerobic Membrane Reactor. *Ecol. Chem. Eng. S* **2022**, *29*, 77–86. [CrossRef]
5. Wang, J.; Zhou, J.; Wang, Y.; Wen, Y.; He, L.; He, Q. Efficient Nitrogen Removal in a Modified Sequencing Batch Biofilm Reactor Treating Hypersaline Mustard Tuber Wastewater: The Potential Multiple Pathways and Key Microorganisms. *Water Res.* **2020**, *177*, 115734. [CrossRef]
6. Liu, S.; Lin, Z.; Zhou, J.; Zhang, Y.; Wang, J.; Zhou, J. Effect of Temperature Downshifts on Performance and Microbial Community Structure on Pilot-Scale Sequencing Batch Biofilm Reactors Treating Hypersaline Wastewater. *Nat. Environ. Pollut. Technol.* **2021**, *20*, 341–347. [CrossRef]
7. Chai, H.; Li, L.; Wei, Y.; Zhou, J.; Kang, W.; Shao, Z.; He, Q. Optimization of Membrane Fouling Process for Mustard Tuber Wastewater Treatment in an Anoxic-Oxic Biofilm-Membrane Bioreactor. *Environ. Eng. Res.* **2016**, *21*, 196–202. [CrossRef]
8. Chen, Y.; Gan, C.J.; Zhou, J. Effect of Environment Factors on Phosphorus Removal Efficiency of Phosphate Reduction System. *Adv. Mater. Res.* **2011**, *255–260*, 2797–2801. [CrossRef]
9. Chen, Y.; Zhou, J.; Long, T.R.; Li, Z.G. Transformation of Phosphorus Forms in the Construction Process of Phosphate Reduction System of Hypersaline and High-Phosphorus Wastewater. In Proceedings of the 2009 International Conference on Energy and Environment Technology, Guilin, China, 16–18 October 2009; IEEE: Piscataway, NJ, USA, 2009; Volume 2, pp. 892–896. [CrossRef]
10. Pendashteh, A.R.; Abdullah, L.C.; Fakhru'L-Razi, A.; Madaeni, S.S.; Zainal Abidin, Z.; Awang Biak, D.R. Evaluation of Membrane Bioreactor for Hypersaline Oily Wastewater Treatment. *Process Saf. Environ. Prot.* **2012**, *90*, 45–55. [CrossRef]
11. de Sousa Rollemberg, S.L.; Mendes Barros, A.R.; Milen Firmino, P.I.; Bezerra dos Santos, A. Aerobic Granular Sludge: Cultivation Parameters and Removal Mechanisms. *Bioresour. Technol.* **2018**, *270*, 678–688. [CrossRef] [PubMed]
12. Han, X.; Jin, Y.; Yu, J. Rapid Formation of Aerobic Granular Sludge by Bioaugmentation Technology: A Review. *Chem. Eng. J.* **2022**, *437*, 134971. [CrossRef]
13. Niu, X.; Han, X.; Jin, Y.; Yue, J.; Zhu, J.; Xie, W.; Yu, J. Aerobic Granular Sludge Treating Hypersaline Wastewater: Impact of PH on Granulation and Long-Term Operation at Different Organic Loading Rates. *J. Environ. Manag.* **2023**, *330*, 117164. [CrossRef]
14. Moussavi, G.; Barikbin, B.; Mahmoudi, M. The Removal of High Concentrations of Phenol from Saline Wastewater Using Aerobic Granular SBR. *Chem. Eng. J.* **2010**, *158*, 498–504. [CrossRef]

15. Ibrahim, A.; Hiripitiyage, Y.; Peltier, E.; Sturm, B.S.M. Use of Halophilic Bacteria to Improve Aerobic Granular Sludge Integrity in Hypersaline Wastewaters. *Environ. Eng. Sci.* **2020**, *37*, 306–315. [CrossRef]
16. Sarvajith, M.; Nancharaiah, Y.V. Biological Nutrient Removal by Halophilic Aerobic Granular Sludge under Hypersaline Seawater Conditions. *Bioresour. Technol.* **2020**, *318*, 124065. [CrossRef] [PubMed]
17. Corsino, S.F.; Capodici, M.; Morici, C.; Torregrossa, M.; Viviani, G. Simultaneous Nitritation-Denitritation for the Treatment of High-Strength Nitrogen in Hypersaline Wastewater by Aerobic Granular Sludge. *Water Res.* **2016**, *88*, 329–336. [CrossRef]
18. Tang, R.; Han, X.; Jin, Y.; Yu, J. Journal of Environmental Chemical Engineering Do Increased Organic Loading Rates Accelerate Aerobic Granulation in Hypersaline Environment ? *J. Environ. Chem. Eng.* **2022**, *10*, 108775. [CrossRef]
19. APHA. *Standard Methods for the Examination of Water and Wastewater*; American Public Health Association: Washington, DC, USA, 2005.
20. Zhang, H.L.; Fang, W.; Wang, Y.P.; Sheng, G.P.; Xia, C.W.; Zeng, R.J.; Yu, H.Q. Species of Phosphorus in the Extracellular Polymeric Substances of EBPR Sludge. *Bioresour. Technol.* **2013**, *142*, 714–718. [CrossRef]
21. Lin, Y.M.; Bassin, J.P.; Van Loosdrecht, M.C.M. The Contribution of Exopolysaccharides Induced Struvites Accumulation to Ammonium Adsorption in Aerobic Granular Sludge. *Water Res.* **2012**, *46*, 986–992. [CrossRef] [PubMed]
22. Hamza, R.A.; Iorhemen, O.T.; Zaghloul, M.S.; Tay, J.H. Rapid Formation and Characterization of Aerobic Granules in Pilot-Scale Sequential Batch Reactor for High-Strength Organic Wastewater Treatment. *J. Water Process Eng.* **2018**, *22*, 27–33. [CrossRef]
23. Shi, Y.; Liu, Y. Evolution of Extracellular Polymeric Substances (EPS) in Aerobic Sludge Granulation: Composition, Adherence and Viscoelastic Properties. *Chemosphere* **2021**, *262*, 128033. [CrossRef] [PubMed]
24. Kent, T.R.; Bott, C.B.; Wang, Z.W. State of the Art of Aerobic Granulation in Continuous Flow Bioreactors. *Biotechnol. Adv.* **2018**, *36*, 1139–1166. [CrossRef] [PubMed]
25. Long, B.; Yang, C.Z.; Pu, W.H.; Yang, J.K.; Liu, F.B.; Zhang, L.; Zhang, J.; Cheng, K. Tolerance to Organic Loading Rate by Aerobic Granular Sludge in a Cyclic Aerobic Granular Reactor. *Bioresour. Technol.* **2015**, *182*, 314–322. [CrossRef]
26. Moy, B.Y.P.; Tay, J.H.; Toh, S.K.; Liu, Y.; Tay, S.T.L. High Organic Loading Influences the Physical Characteristics of Aerobic Sludge Granules. *Lett. Appl. Microbiol.* **2002**, *34*, 407–412. [CrossRef]
27. Song, W.; Xu, D.; Bi, X.; Ng, H.Y.; Shi, X. Intertidal Wetland Sediment as a Novel Inoculation Source for Developing Aerobic Granular Sludge in Membrane Bioreactor Treating High-Salinity Antibiotic Manufacturing Wastewater. *Bioresour. Technol.* **2020**, *314*, 123715. [CrossRef]
28. Wang, L.; Cui, Y.-W.; Jian, L.; Yao, J.-L. Spontaneous Granulation of Moderately Halophilic Sludge Inoculated with Saltern Sediments from Single Granule into Multi-Granule Aggregation. *Environ. Res.* **2022**, *216*, 114813. [CrossRef]
29. Wang, B.B.; Luo, Q.; Li, H.J.; Yao, Q.; Zhang, L.; Zou, J.T.; He, F. Characterization of Aerobic Granules Formed in an Aspartic Acid Fed Sequencing Batch Reactor under Unfavorable Hydrodynamic Selection Conditions. *Chemosphere* **2020**, *260*, 127600. [CrossRef] [PubMed]
30. Liu, Y.; Tang, H.; Lin, Z.; Xu, P. Mechanisms of Acid Tolerance in Bacteria and Prospects in Biotechnology and Bioremediation. *Biotechnol. Adv.* **2015**, *33*, 1484–1492. [CrossRef] [PubMed]
31. Liu, Y.; Chen, Y.; Zhou, Q. Effect of Initial PH Control on Enhanced Biological Phosphorus Removal from Wastewater Containing Acetic and Propionic Acids. *Chemosphere* **2007**, *66*, 123–129. [CrossRef]
32. Li, Y.; Chapman, S.J.; Nicol, G.W.; Yao, H. Nitrification and Nitrifiers in Acidic Soils. *Soil Biol. Biochem.* **2018**, *116*, 290–301. [CrossRef]
33. Li, A.J.; Yang, S.F.; Li, X.Y.; Gu, J.D. Microbial Population Dynamics during Aerobic Sludge Granulation at Different Organic Loading Rates. *Water Res.* **2008**, *42*, 3552–3560. [CrossRef]
34. Jiang, Y.; Wei, L.; Yang, K.; Shi, X.; Wang, H. Rapid Formation of Aniline-Degrading Aerobic Granular Sludge and Investigation of Its Microbial Community Succession. *J. Clean. Prod.* **2017**, *166*, 1235–1243. [CrossRef]
35. Zhang, A.; Gao, C.; Chen, T.; Xie, Y.; Wang, X. Treatment of Fracturing Wastewater by Anaerobic Granular Sludge: The Short-Term Effect of Salinity and Its Mechanism. *Bioresour. Technol.* **2022**, *345*, 126538. [CrossRef] [PubMed]
36. Xiong, W.; Wang, S.; Zhou, N.; Chen, Y.; Su, H. Granulation Enhancement and Microbial Community Shift of Tylosin-Tolerant Aerobic Granular Sludge on the Treatment of Tylosin Wastewater. *Bioresour. Technol.* **2020**, *318*, 124041. [CrossRef]
37. Li, J.; Ma, Z.; Gao, M.; Wang, Y.; Yang, Z.; Wang, X. Enhanced Aerobic Granulation at Low Temperature by Stepwise Increasing of Salinity. *Sci. Total Environ.* **2020**, *722*, 137660. [CrossRef] [PubMed]
38. Zou, Y.; Zhong, Y.; Huang, L.; Xu, W.; Wu, Y.; Gao, J.; Zhong, K.; Gao, H. Effects of Brown Sugar Addition and Fermentation Time on Metabolites and Microbial Communities of Yibin Yacai. *LWT* **2022**, *165*, 113720. [CrossRef]
39. Zhang, B.; Wu, L.; Shi, W.; Zhang, Z.; Lens, P.N.L. A Novel Strategy for Rapid Development of a Self-Sustaining Symbiotic Algal-Bacterial Granular Sludge: Applying Algal-Mycelial Pellets as Nuclei. *Water Res.* **2022**, *214*, 118210. [CrossRef] [PubMed]
40. Shi, X.; Li, J.; Wang, X.; Zhang, X.; Tang, L. Effect of the Gradual Increase of Na2SO4 on Performance and Microbial Diversity of Aerobic Granular Sludge. *J. Environ. Manag.* **2021**, *292*, 112696. [CrossRef]
41. He, Q.; Zhang, W.; Zhang, S.; Zou, Z.; Wang, H. Performance and Microbial Population Dynamics during Stable Operation and Reactivation after Extended Idle Conditions in an Aerobic Granular Sequencing Batch Reactor. *Bioresour. Technol.* **2017**, *238*, 116–121. [CrossRef]
42. Wang, Z.J.; Liu, Q.Q.; Zhao, L.H.; Du, Z.J.; Chen, G.J. Bradymonas Sediminis Gen. Nov., Sp. Nov., Isolated from Coastal Sediment, and Description of Bradymonadaceae Fam. Nov. and Bradymonadales Ord. Nov. *Int. J. Syst. Evol. Microbiol.* **2015**, *65*, 1542–1549. [CrossRef]

43. Jiang, Y.; Shi, X.; Ng, H.Y. Aerobic Granular Sludge Systems for Treating Hypersaline Pharmaceutical Wastewater: Start-up, Long-Term Performances and Metabolic Function. *J. Hazard. Mater.* **2021**, *412*, 125229. [CrossRef]
44. Ou, D.; Li, H.; Li, W.; Wu, X.; Wang, Y.Q.; di Liu, Y. Salt-Tolerance Aerobic Granular Sludge: Formation and Microbial Community Characteristics. *Bioresour. Technol.* **2018**, *249*, 132–138. [CrossRef] [PubMed]
45. Zhang, X.; Chen, A.; Zhang, D.; Kou, S.; Lu, P. The Treatment of Flowback Water in a Sequencing Batch Reactor with Aerobic Granular Sludge: Performance and Microbial Community Structure. *Chemosphere* **2018**, *211*, 1065–1072. [CrossRef] [PubMed]
46. Zeng, D.; Miao, J.; Wu, G.; Zhan, X. Nitrogen Removal, Microbial Community and Electron Transport in an Integrated Nitrification and Denitrification System for Ammonium-Rich Wastewater Treatment. *Int. Biodeterior. Biodegrad.* **2018**, *133*, 202–209. [CrossRef]
47. Chen, J.; Han, Y.; Wang, Y.; Gong, B.; Zhou, J.; Qing, X. Start-up and Microbial Communities of a Simultaneous Nitrogen Removal System for High Salinity and High Nitrogen Organic Wastewater via Heterotrophic Nitrification. *Bioresour. Technol.* **2016**, *216*, 196–202. [CrossRef]
48. Huang, J.L.; Wang, H.H.; Alam, F.; Cui, Y.W. Granulation of Halophilic Sludge Inoculated with Estuarine Sediments for Saline Wastewater Treatment. *Sci. Total Environ.* **2019**, *682*, 532–540. [CrossRef]
49. Li, T.; Li, Y.; Li, M.; Wang, N.; Sun, Z.; Li, X.; Li, B. Effects of Sulfamethoxazole on Nitrogen Transformation and Antibiotic Resistance Genes in Short-Cut Nitrification and Denitrification Process Treating Mariculture Wastewater. *Chem. Eng. J.* **2023**, *454*, 140517. [CrossRef]